Research Article

Journal of Environmental Nanotechnology

Hydrothermal Synthesis and Enhanced Corrosion Inhibition Activity of CdS QDs towards Zn Surface

K. Kandasamy[1], P. Rajasingh[2*]

[1]Department of Chemistry, K.S.R College of Arts and Science for Women, Tiruchengode, TN, India

[2]Department of Chemistry, Chikkanna Government Arts College, Tiruppur, TN, India

Received: 10.04.2021 Accepted: 05.05.2021 Published: 30-06-2021

*sprajasingh@gmail.com

ABSTRACT

The hydrothermal method was used to synthesize hexagonal 3-5 nm Cadmium Sulfide Quantum Dots (CdS QDs) with *Delonix elata* leaves' aqueous extract as a capping agent. The synthesized CdS QDs were characterized by FTIR, UV-Vis, XRD, FE-SEM spectroscopies. The anticorrosion activity of the CdS QDs-coated Zn plate was exanimated under 1 M HCl, 6 M KOH, 3.5% NaCl electrolytic medium. The best corrosion resistance was achieved through the application of the CdS QDs coating on the Zn metal surface.

Keywords: Anticorrosion activity; *Delonix elata*; Hexagonal CdS QDs; Hydrothermal method.

1. INTRODUCTION

Zinc-based alloys and zinc oxide are used in various applications in the automobile, construction, light industry, batteries and other industries. High quantities of zinc are used to produce die-castings in the automobile, electrical and hardware industries. Zinc oxide is extensively used in the production of paints, rubber, cosmetics, inks, pharmaceuticals and electrical equipment (Raja *et al.* 2016). Originally, a fresh zinc surface corrodes fairly quickly until it is enclosed with protective films. In tremendously polluted industrial atmospheres, the corrosion rate may rise with continued exposure. The corrosion rate in marine atmospheres has been found to decrease as the time of exposure increases (Quintana *et al.* 1996). *Delonix elata* leaves' aqueous extract has a natural capacity to act as a promising capping, stabilizing and reducing agent in the synthesis of quantum dots. Through green synthetic protocols, *Delonix elata* leaf aqueous extract is used as an eco-friendly solvent and excellent capping agent in the fabrication of stable QDs. The plant extract-mediated cadmium sulfide quantum dots (CdS QDs) can be biocompatible and nontoxic (Abiola *et al.* 2010). They are extremely promising organic corrosion inhibitors and can act as photosensitizers for treating cancer. The high toxicity of chemical corrosion inhibitors compelled the researchers to search for green corrosion inhibitors as they are biodegradable and do not contain heavy metals and toxic substances (Gerengi *et al.* 2012). Additionally, plant products are inexpensive, readily available, renewable and non-toxic. Plants contain a lot of phytochemicals like tannins, flavonoids, alkaloids, organic amino acids, pigments and dyes (Rani *et al.* 2012).

There is only a little information available about the processes of corrosion of zinc exposed to environmental conditions. So herein, CdS QDs were designed as a corrosion inhibitor and synthesized using *Delonix elata* leaves aqueous extract via a one-pot hydrothermal protocol.

2. EXPERIMENTAL SECTION

2.1 Materials

Reagent grade cadmium chloride ($CdCl_2.H_2O$), sodium sulfide ($Na_2S.H_2O$), polyvinylidene fluoride (PVDF), N-methyl-2-pyrrolidone (NMP) purchased were of the highest purity available and used without any further purification.

2.2 Synthesis of *Delonix elata* CdS QDs by Hydrothermal method

The *Delonix elata* leaves' aqueous extract was prepared by using the procedure given in the literature (Kandasamy *et al.* 2020a; Sudha *et al.* 2021).

2.3 Characterization

XRD pattern of CdS QDs samples was characterized by CuKα (λ=1·5406 Å) radiation generated at 40 KeV, 40 mA and scanned in the 2θ range from 10 to 80°. At room temperature, an FT-IR spectrum was recorded in the range of 4000 to 400 cm^{-1}. A Cary 5000 UV-Vis spectrophotometer has been used to evaluate the UV-visible maximum absorption spectrum of CdS QDs. A field transmission electron microscope was used to examine the scanning electron images.

2.4 Electrochemical measurements

A pure zinc metal plate was used to study the corrosive inhibition behavior. The Zn metal plate was consequently polished with 1 mm silicon carbide grit papers and cleaned with acetone. The synthesized *Delonix elata* CdS QDs by Hydrothermal method (DCH) was mixed with PVDF and NMP at 80:15:5 weight ratio to prepare a slurry. The slurry was further coated over on the metal surface of the Zn plate using the Doctor blade technique. The coated plate was dried in an oven at 353 K for 1 hour and then used for corrosion studies.

3. RESULT AND DISCUSSION

3.1 XRD Analysis

Fig. 1 (a) shows that almost all of the peaks in the prepared samples can be correctly indexed into the hexagonal CdS phase (JCPDS card No. 41-1049). The Wurtzite (hexagonal) phase is the most stable one compared to the others and also the easiest to synthesize. The peaks at 2θ = 25.30°, 27.04°, 28.34°, 36.64°, 44.22°, 48.26° and 52.31° are corresponding to the (1 0 0), (0 0 2), (1 0 1), (1 0 2), (1 1 0) and (1 0 3), respectively (Kandasamy *et al.* 2020).

3.2 FT-IR Spectroscopy

The FTIR spectrum of the DCH sample was shown in Fig. 1 (b). The bands at 1603 cm^{-1}, 1390 cm^{-1}, 1254 cm^{-1}, and 1071 cm^{-1} correspond to the –C=O stretching, –C=H bending, –C-O and –C-N stretching vibrations; the absorption bands in 834 cm^{-1} and 543 cm^{-1} regions correspond to the –C-Cl and –C-Br halide functional groups. The peak at 620 cm^{-1} confirms the formation of CdS QDs (Sudha *et al.* 2021).

3.3 UV-Vis Spectrometer

The optical absorption of DCH was investigated by the UV-Vis absorption spectrum. It can be observed from Fig. 1 (c) that the DCH sample at λ = 463 nm corresponds to the photo-absorption edge of CdS nanocrystals. The bandgap energy value is 2.37 eV (Kandasamy *et al.* 2020b).

3.4 FE-SEM Analysis

The morphologies of DCH were observed using FE-SEM. The image in Fig. 1(d) demonstrates that the DCH involves spherical shape particles with an average diameter of 5-7 nm. The size of DCH detected in FE-SEM images corresponds to the XRD results. The similarities in particle size and thus the formation of CdS QDs are confirmed by comparing XRD and FE-SEM results (Lei *et al.* 2018).

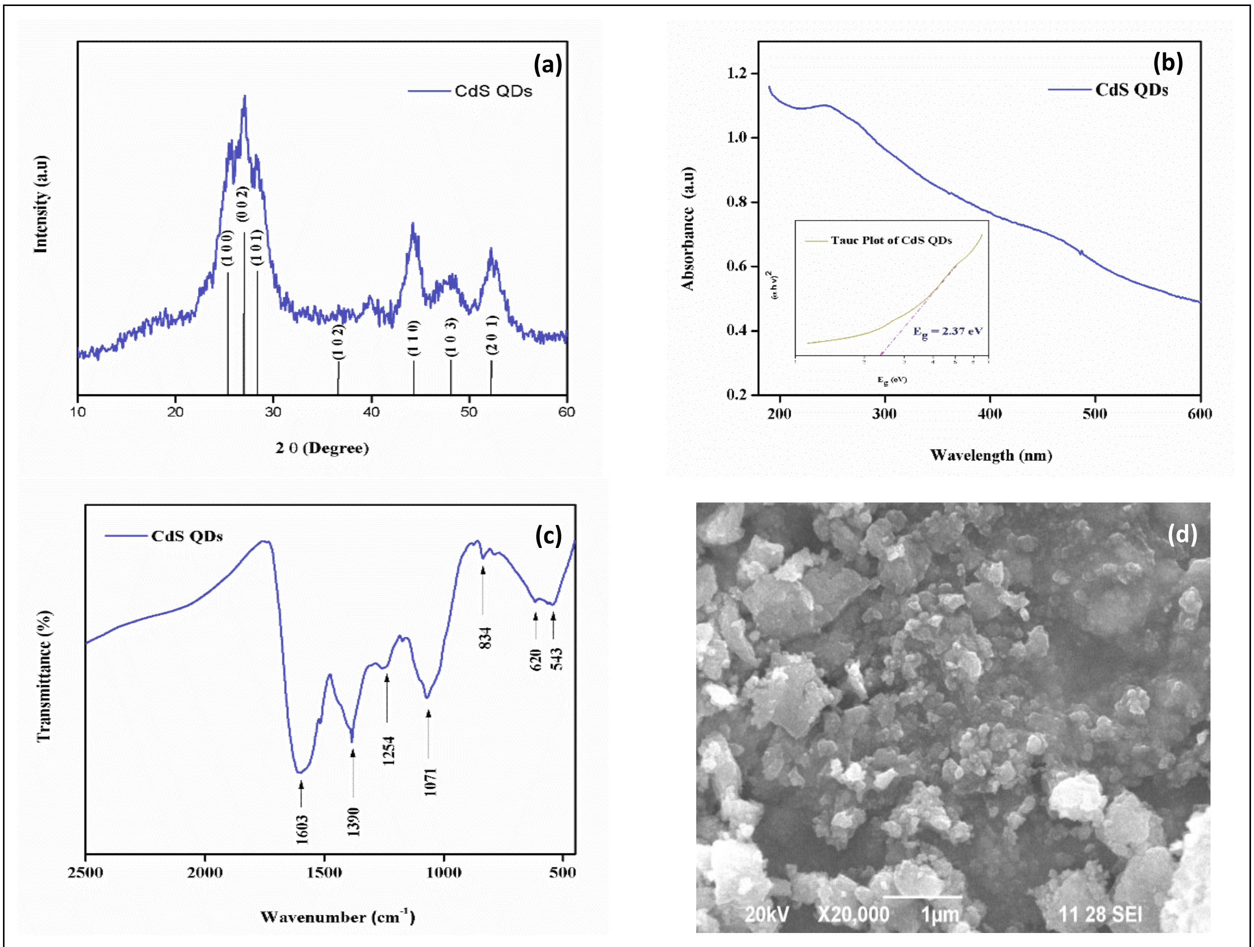

Fig. 1: (a) XRD (b) FTIR (c) UV-Vis (d) FE-SEM Spectra for DCH sample

3.5 Tafel Curve-based Measurement of DCH

The Tafel plots of pure Zn and DCH corrosion inhibitor/Zn plate in three different aqueous electrolytes are shown in Fig.2 (a) 1M HCl (b) 3.5% NaCl and (c) 6 M KOH. The corrosion rate was observed on pure Zn plates and DCH corrosion inhibitor-coated Zn plates for all the electrolytes with -1.4 V to – 0.4 V. The corrosion potential value of the DCH/Zn plate is moved towards the anodic region compared to the pure Zn plate. The corrosion rate (mm/year) measured from the Tafel curve for Zn plate is 1.4356 (mm/year) and DCH/ Zn plate is 0.3821 (mm/year), for 1M HCl aqueous electrolyte (Table 1).

Similarly, the corrosion rate (mm/year) of Zn plates are 2.0642 and 1.3465 and DCH/Zn plates are 1.6881 and 0.3189 (mm/year) for 3.5% NaCl and 6 M KOH, respectively. The DCH has a lower corrosion rate than pure Zn, clearly indicating that the improved corrosion resistance is due to the coating of DCH corrosion inhibitor over Zn metal surface. The corrosion-preventive nature of the DCH sample has been demonstrated in this study (Selvam *et al.* 2016).

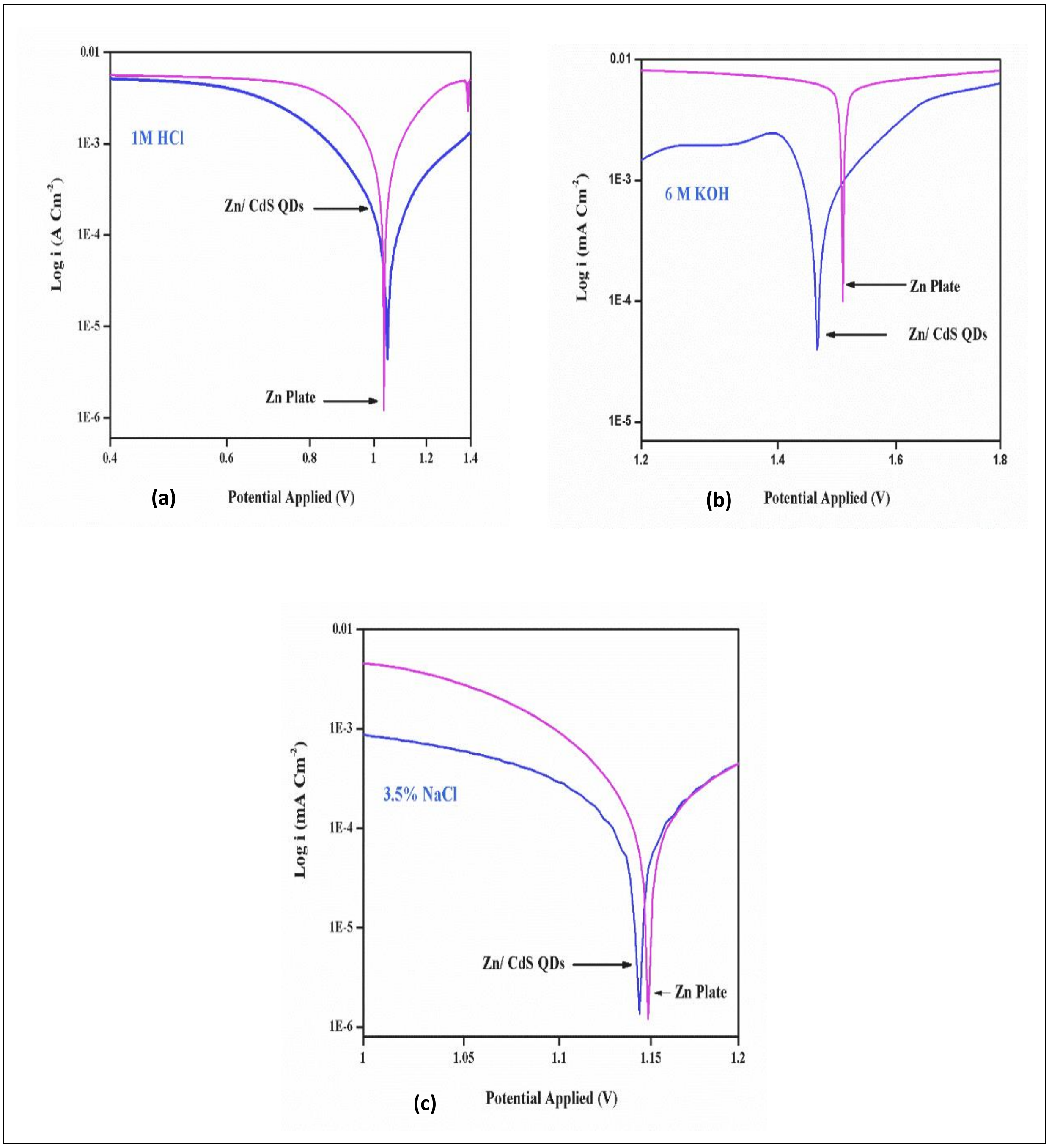

Fig. 2: (a) 1 M HCl (b) 3.5 % NaCl (c) 6 M KOH Tafel curves for DCH sample

Table 1. The computed values of Tafel curves in 1 M HCl, 3.5 % NaCl and 6 M KOH electrolytes

Electrolyte	Sample	Corrosion potential E_{corr} (mV)	Corrosion current I_{corr} (ACm^{-2})	Corrosion rate (mm/year)
1M HCl	Pure Zn DCH/ Zn plate	-1.1002 -1.0475	0.9697 0.3288	1.4356 0.3821
3% NaCl	Pure Zn DCH /Zn plate	-1.2487 -1.1433	1.6998 1.5520	2.0642 1.6881
6M KOH	Pure Zn DCH/ Zn plate	-1.6850 -1.4642	1.2554 0.2745	1.3465 0.3189

3.5 Tafel curve measurement of DCH

The Tafel plots of pure Zn and DCH corrosion inhibitor/Zn plate in three different aqueous electrolytes were shown in Fig.2 (a) 1M HCl (b) 3.5% NaCl and (c) 6 M KOH. The corrosion rates were observed on pure Zn plates and DCH corrosion inhibitor-coated Zn plates for all the electrolytes with -1.4 V to – 0.4 V. The corrosion potential value of DCH/Zn plate is moved towards the anodic region compared to the pure Zn plate. The corrosion rates (mm/year) measured from the Tafel curve for Zn plate is 1.4356 (mm/year) and DCH/Zn plate is 0.3821 (mm/year) for 1M HCl aqueous electrolyte (Table 1). Similarly, the corrosion rates (mm/year) of Zn plates are 2.0642 and 1.3465 and DCH/Zn plates are 1.6881 and 0.3189 (mm/year) for 3.5% NaCl and 6 M KOH, respectively. The DCH has a lower corrosion rate than pure Zn, clearly indicating that the improved corrosion resistance is due to the coating of DCH corrosion inhibitor over Zn metal surface. The corrosion-preventive nature of the DCH sample has been demonstrated in this study (Selvam *et al.* 2016).

4. CONCLUSION

A successful method has been developed to synthesize CdS QDs using *Delonix elata* leaves' aqueous extract by the hydrothermal method. The CdS QDs were tested in the corrosion inhibition activity of the Zn surface. The hexagonal (Wurtzite) phase and spherical shape of CdS QDs were confirmed by XRD and FE-SEM, respectively. The as-synthesized material coated on zinc metal surface provided good corrosion protection. The hydrothermal method of synthesis may change the morphology of the product, thereby improving its corrosion activity.

FUNDING

This research received no specific grant from any funding agency in the public, commercial, or not-for-profit sectors.

CONFLICTS OF INTEREST

The authors declare that there is no conflict of interest.

REFERENCES

Abiola, O. K. and James, A. O., The effects of Aloe vera extract on corrosion and kinetics of corrosion process of zinc in HCl solution, *Corros. Sci.*, 52(2), 661–664 (2010). https://dx.doi.org/10.1016/j.corsci.2009.10.026

Gerengi, H. and Sahin, H. I., *Schinopsis lorentzii* extract as a green corrosion inhibitor for low carbon steel in 1 M HCl solution, *Indian Eng. Chem. Res.*, 51(2), 780–787 (2012). https://dx.doi.org/10.1021/ie201776q

Kandasamy, K., Surendhiran, S., Syed Khadar, Y. A. and Rajasingh, P., Ultrasound-assisted microwave synthesis of CdS/MWCNTs QDs: A material for photocatalytic and corrosion inhibition activity, *Mater Today Proc*.,(2020). https://dx.doi.org/10.1016/j.matpr.2020.07.080

Kandasamy, K., Venkatesh, M., Syed Khadar, Y. A. and Rajasingh, P., One-pot green synthesis of CdS quantum dots using *Opuntia ficus-indica* fruit sap, *Mater. Today Proc.*, 26, 3503–3506 (2020b). https://dx.doi.org/10.1016/j.matpr.2019.06.003

Lei, R., Ni, H., Chen, R., Gu, H., Zhang, B. and Zhan, DW., Hydrothermal synthesis of CdS nanorods anchored on α-Fe_2O_3 nanotube arrays with enhanced visible-light-driven photocatalytic properties, *J. Colloid Interface Sci.*, 514, 496–506 (2018). https://dx.doi.org/10.1016/j.jcis.2017.12.061

Quintana, P., Veleva, L., Cauich, W., Pomes, R. and Peña, J. L., Study of the composition and morphology of initial stages of corrosion products formed on Zn plates exposed to the atmosphere of southeast Mexico, *Appl. Surf. Sci.*, 99(4), 325–334 (1996). https://dx.doi.org/10.1016/0169-4332(96)00597-1

Raja, P. B., Ismail, M., Ghoreishiamiri, S., Mirza, J., Ismail, M. C., Kakooei, S. and Rahim, A. A., Reviews on corrosion inhibitors: A short view, *Chem. Eng. Commun.*, 203(9), 1145–1156 (2016). https://dx.doi.org/10.1080/00986445.2016.1172485

Rani, B. E. A. and Basu, B. B. J., Green inhibitors for corrosion protection of metals and alloys: An overview, *Int. J. Corros.*, 2012, 01–15 (2012). https://dx.doi.org/10.1155/2012/380217

Selvam, M., Saminathan, K., Siva, P., Saha, P. and Rajendran, V., Corrosion behavior of Mg/graphene composite in aqueous electrolyte, *Mater. Chem. Phys.*, 172, 129–136 (2016). https://dx.doi.org/10.1016/j.matchemphys.2016.01.051

Sudha, M., Surendhiran, S., Gowthambabu, V., Balamurugan, A., Anandarasu, R., Syed Khadar, Y. A. and Vasudevan, D., Enhancement of corrosive-resistant behavior of Zn and Mg metal plates using biosynthesized nickel oxide nanoparticles, *J. Bio-Tribo-Corrosion.*, 7(2), 60 (2021). https://dx.doi.org/10.1007/s40735-021-00492-w